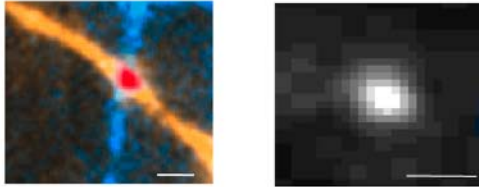
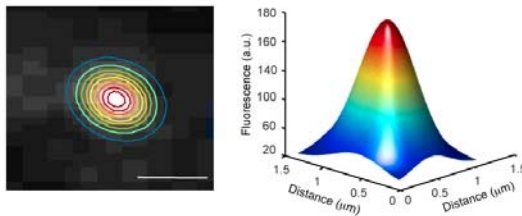


1 Measure recycling pool size

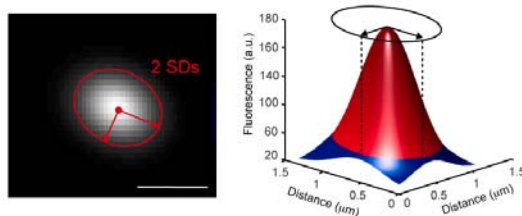
A Select synapse



B Fit 2-D Gaussian curve

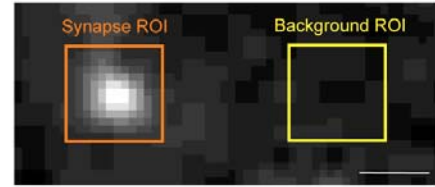


C Define border and integrate fluorescence

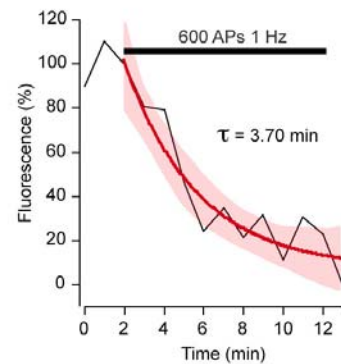


2 Measure FM-dye loss

D Define region of interest and local background area



E Measure fluorescence for each frame and fit single exponential



3 Calculate *release probability*

$$p_r = \frac{0.63 \times \text{no. recycling pool vesicles}}{60 \text{ APs} \cdot \text{min}^{-1} \times \tau \text{ min}}$$

Figure S1. Estimating release probability using FM-dyes. (A) Synapses of interest were selected based on the apposition of the FM-dye signal with the Alexa-dye filled axon (blue) and/or dendrite (orange) (left). For display purposes the independent fluorescence signals from the cell processes were assembled into one RGB image and rendered to the colours shown. The FM-dye fluorescence was then overlaid as a separate RGB layer and digitally blended in Photoshop CS2 (Adobe Systems Inc.). All quantifications were made using raw images (right). (B) To estimate the size of the recycling pool the initial FM-dye puncta fluorescence was first fit with a 2-D Gaussian. (C) The synapse border was defined as 2 SDs from the centre of the fit and the total fluorescence quantified by integrating the fit within this limit. The mean integrated fluorescence for all the synapses in a connection was assumed to correspond to the reported average recycling pool size for hippocampal synapses at room temperature of 127 vesicles (Ryan et al, 1997). This was then used to convert fluorescence into number of vesicles for each individual synapse. (D) To measure the stimulation evoked FM-dye loss, a region of interest (ROI) was defined around a punctum and an equivalent region positioned adjacent to it to measure the local background signal. Mean fluorescence was calculated for each region and the background signal subtracted from the synapse signal for every frame. (E) Destaining kinetics were obtained by fitting a single exponential curve to the FM-dye fluorescence loss. Release probability was then calculated as the number of vesicles released at the time constant (63% of initial pool) divided by the number of APs at this point. This only takes into account the release of stained vesicles, and therefore may lead to an underestimation of the true value of release probability due to the re-release of vesicles that have already lost FM-dye.

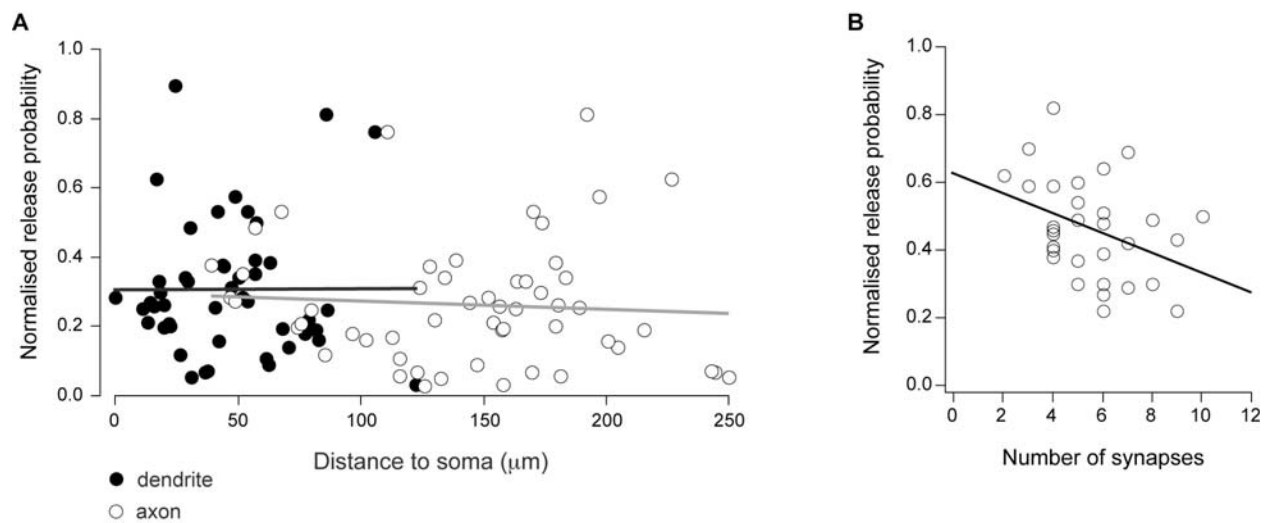


Figure S2. Spatial analysis of release probability. (A) Release probability measured by FM-dye destaining rate for all synapses along dendritic or axonal branches, shows no relationship with the morphological distance from the soma. Lines are separate linear fits to the data for distance measured along axons (gray) and dendrite (black). (B) There is an inverse relationship between synapse density in the dendrite and release probability. Line is a linear fit to the data, $R = -0.38$. In both panels, p_i has been normalized by the mean of each cell.

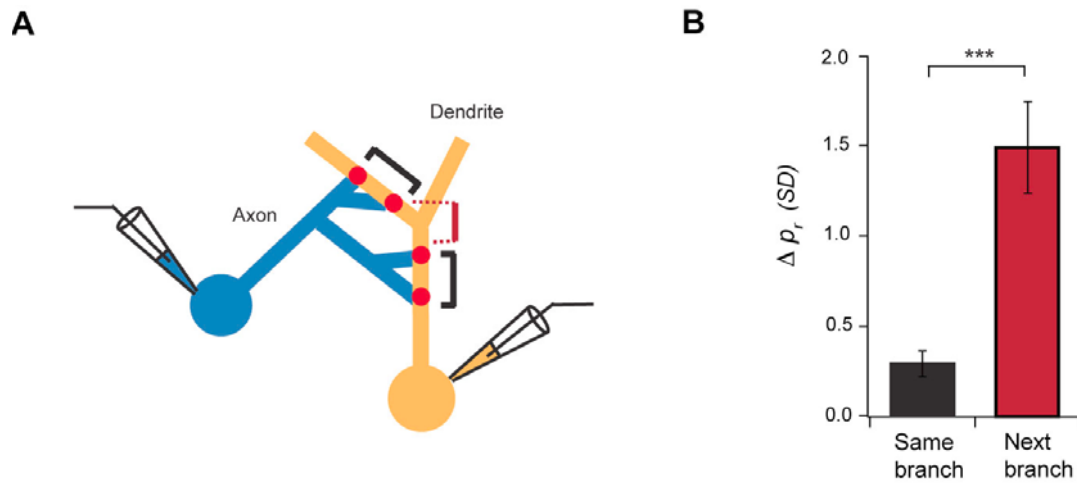


Figure S3. Dendritic branchpoint p_r analysis. From the dataset presented in Figure 2, cases where synapses from the same input were found in two consecutive dendritic branches were selected, and analysed for similarity in release probability. (A) Cartoon illustrating the comparisons made. Black bars indicate “same branch” comparison and red bar shows “next branch” comparison. (B) Summary data for all cases analysed. $N = 5$ dendrites (each dendrite includes one parent and one daughter branch) from 4 cell pairs, $P < 0.0001$.

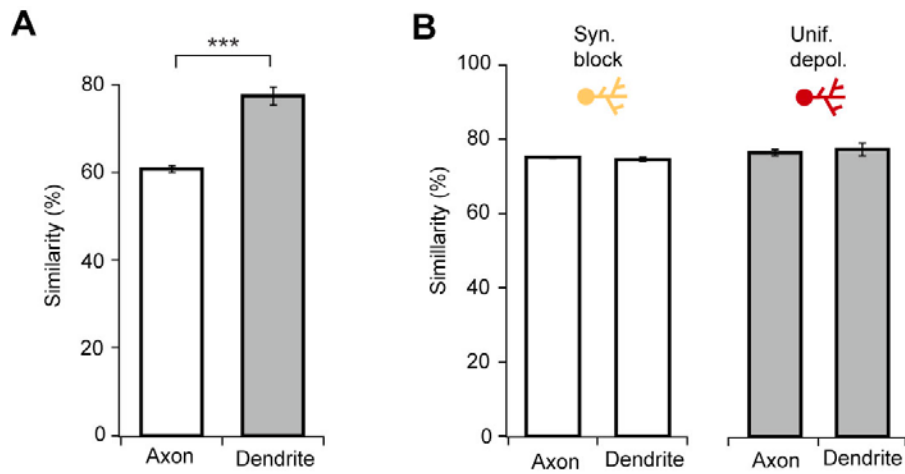


Figure S4. Recycling pool sizes mimics p_r results. (A) Same type of comparison as in Figure 1G, except instead of calculating p_r differences between synapses, a measure of similarity was obtained by calculating the total fluorescence intensity ratio between synapse pairs. For a given synapse pair, the lowest number was always chosen as the denominator, so the measure varies between 0 and 100%. As found for release probability, recycling pool sizes of synapses made on the same dendritic branch are very similar. (B) After imposing a spatially uniform input to the dendrite as in Fig. 5F, recycling pool sizes become uniform throughout the whole dendritic tree regardless of whether they belong to the same axon or not. Pool sizes were measured by fitting a 2-D Gaussian curve to the initial FM-dye fluorescence after KCl stimulation.

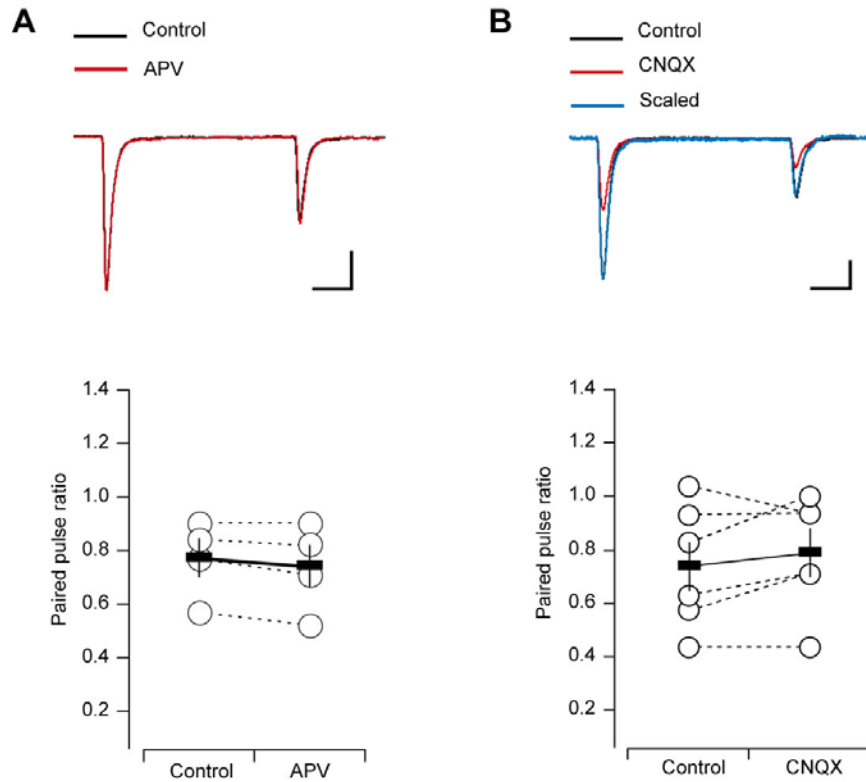


Figure S5. Paired pulse response provides no evidence for neurotransmitter release modulation by presynaptic NMDA and AMPA receptors. (A) Top, superimposed paired-pulse example traces before and after perfusion of 50 μM APV (average of 20). Bottom, summary plot (bottom, $n = 4$) shows no change in PPR in the presence of APV (control, 0.77 ± 0.07 , APV, 0.74 ± 0.08 , paired t -test, $P = 0.0994$). (B) Top, example traces of paired-pulse responses in control and during perfusion of a sub-saturating concentration of CNQX (400 nM). Blue trace is the response in CNQX peak-scaled to the control EPSC to illustrate the lack of change in kinetics. Bottom, summary of 6 connections shows no change in PPR with application of CNQX (control, 0.74 ± 0.09 , CNQX, 0.79 ± 0.09 , paired t -test $P = 0.2822$). Scale bars, a, 10 ms, 200 pA, b, 10 ms, 100 pA. Error bars are \pm s.e.m.

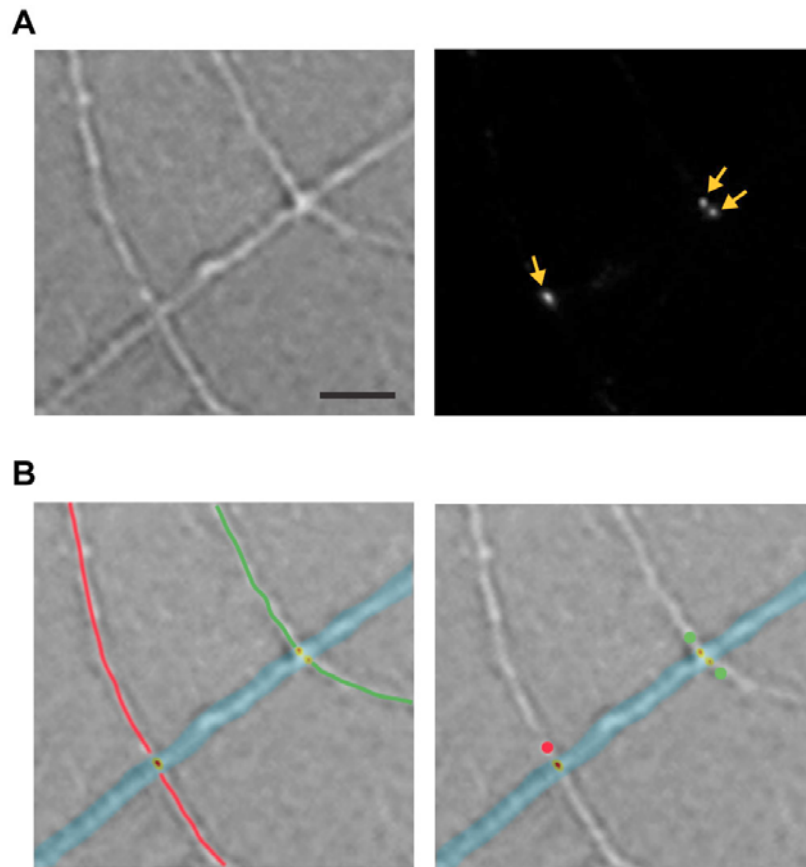


Figure S6. Example of axonal tracing for local stimulation experiments shown in Fig. 6. To identify the input origin of FM-dye labelled synapses, DIC images (A, left) and matching FM-dye images (A, right) were used. To help the process of tracing, the contrast of FM-dye images was sometimes enhanced to reveal the background membrane staining and allow visualization of cell processes. Due to the low density of cells and processes in the cultures, it was possible to follow the axons of synapses of interest back to their origin, and classify synapses according to their presynaptic origin (B). Scale bar, 5 μm .

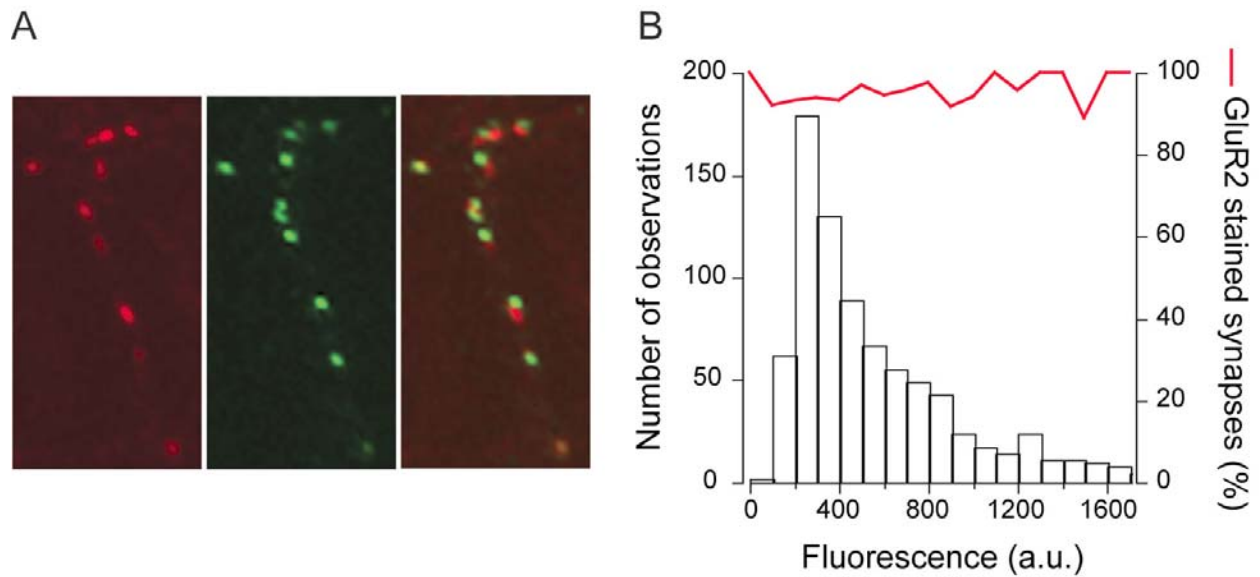


Figure S7. The population of synapses studied is mature. (A) Presynaptic terminals were labeled with stimulation (30 APs, 1 Hz) in the presence of FM4-64 (left panel), and mature synapses identified by their close apposition to GluR2 clusters (center panel, right shows overlay). (B) A histogram constructed with the total FM4-64 fluorescence intensity measured for each synapse ($n = 820$). The percentage of synapses in each histogram bin apposed to GluR2 is indicated by the red line. On average, more than 90% of FM-dye labelled synapses were apposed to GluR2, indicating a high degree of synapse maturation in the cultures used for experiments (Pickard et al, 2000). Also, there is no relation between the integrated FM-dye fluorescence, which is proportional to release probability, and the fraction of GluR2 labelling. This excludes the possibility that synapses with different release probabilities are in different developmental stages.

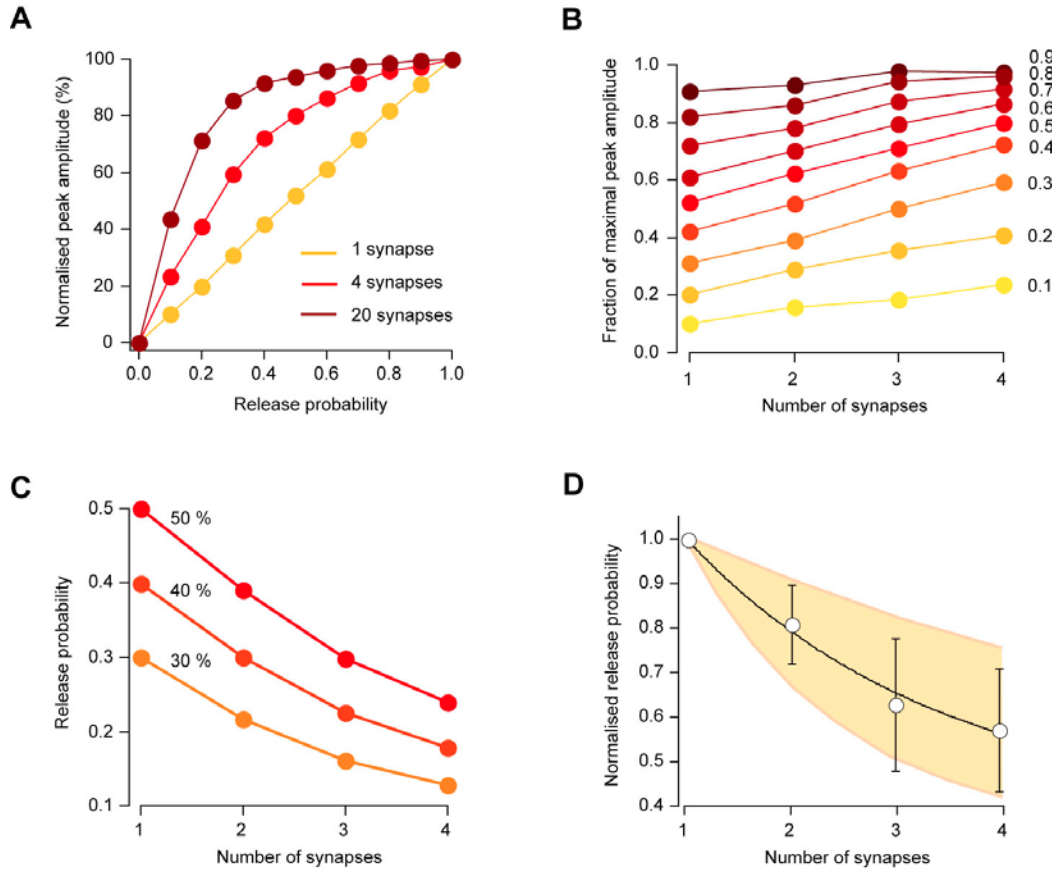


Figure S8. Theoretical relationship between release probability and the number of synchronously activated synapses. Simulations of a CA1 pyramidal neuron were performed using the NEURON simulation program (version 5.9, see Hines and Carnevale, 1997). The realistic model of a CA1 neuron was the same as in Gasparini et al, 2004, and was downloaded from the Senselab database (<http://senselab.med.yale.edu>). All the biophysical parameters of the model were kept the same, including sodium, delayed rectifier, A-type potassium and non-inactivating, nonspecific cation currents in all compartments. Excitatory synapses were modelled as AMPA conductances using a single exponential function [the ExpSyn() built-in function in NEURON, modified to include an adjustable release probability to the stimulus] with a 1 ms time constant, a reversal potential of 0 mV and a peak conductance of 1.5 nS. A variable number of synapses with the same p_r were placed evenly around the centre (spacing 1 μ m) of a randomly selected apical dendrite. All other dendrites were left without any synaptic input. Peak EPSP amplitude was recorded at the dendrite. (A) Plot of peak EPSP amplitude normalised to the response when $p_r = 1$ against release probability for three different numbers of synapses in the dendrite. Synapses were stimulated synchronously. As the number of synapses increases, the relation between p_r and EPSP amplitude becomes sub-linear due to decreased input resistance and reduced driving force. (B) For a given value of p_r (coloured lines, value of p_r indicated for each one), increasing the number of synapses in the dendrite leads to responses closer to saturation, defined as the peak amplitude when $p_r = 1$. (C) To maintain a constant position in the dynamic range with different numbers of synapses, release probability has to decrease as the number of synapses increases. The plot shows the necessary change in p_r required to maintain three different levels of saturation (indicated by different coloured lines). (D) Shaded area shows the theoretical changes in p_r to maintain saturations between 10% (lower limit) to 90% (upper limit) with increasing numbers of synapses. Experimental data is superimposed and shows a very good agreement with the predicted magnitude and rate of change of release probability. Line is a single exponential fit to the data. Error bars are \pm s.e.m.

Supplemental References

Gasparini, S., Migliore, M., and Magee, J.C. (2004). On the initiation and propagation of dendritic spikes in CA1 pyramidal neurons. *J. Neurosci.* 24, 11046–11056.

Hines, M.L., and Carnevale, N.T. (1997). The NEURON simulation environment. *Neural Comput.* 9, 1179–1209.

Pickard, L., Noel, J., Henley, J.M., Collingridge, G.L., and Molnar, E. (2000). Developmental changes in synaptic AMPA and NMDA receptor distribution and AMPA receptor subunit composition in living hippocampal neurons. *J. Neurosci.* 20, 7922–7931.

Ryan, T.A., Reuter, H., and Smith, S.J. (1997). Optical detection of a quantal presynaptic membrane turnover. *Nature* 388, 478–482.